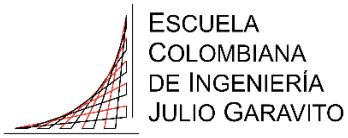

Advanced State of Charge Management in Lithium-ion Parallel Battery Cells

Nicolas Castro Gomez

Juan Camilo Ospina Sanchez

Escuela Colombiana de Ingeniería Julio Garavito

Electronic Engineering

Bogota D.C., Colombia

2024

Advanced State of Charge Management in Lithium-ion Parallel Battery Cells

Nicolas Castro Gomez

Juan Camilo Ospina Sanchez

Directed project seeking emphasis line:

Electronics design and integration

Project Supervisor:

Johnny Alexander Arévalo López

Escuela Colombiana de Ingeniería Julio Garavito

Electronic Engineering

Bogota D.C., Colombia

2024

Abstract

This paper is dedicated to present a functional Ion-lithium battery cell balancing prototype that enhances the self-balancing batteries behavior introducing an innovative and efficient approach. Since parallel cell configurations are commonly used in commercial battery packs, the research primary goal is to develop an introductory model that can be easily adapted for more complex battery setups in future applications. Additionally, it will be used as a test circuit for analyzing battery charge and discharge behaviors.

1. Contents

2. Acronyms

ADC: Analog to digital converter

BMS: Battery management system

BPNN: Backpropagation neural network

CCCV: Constant current constant voltage

CTCV: Constant temperature constant voltage

IC: Integrated circuit

OCV: Open circuit voltage

PCB: Printed circuit board

SOC: State of charge

SOH: State of health

3. Introduction

The Lithium-ion battery industry encounters various problems that affect the efficiency and performance within their products. Some of them include battery degradation, excessive heating and unnecessary waste of energy. Hemavathi in [1] refers that in the realm of Li-ion batteries, it is crucial to maintain precise control over variables at both the individual battery cell and the larger pack level. This meticulous control is imperative to ensure the safe operation of the battery system. The oversight and protection of these control variables falls under the responsibility of the battery management system (BMS).

One issue with lithium-ion batteries occurs when their State of Charge (SOC) isn't within the proper range, which can either be over or under the safe operational limits, it causes undesired electrochemical reactions such as electrolyte decomposition, described by Yuqing Chen, et al. [8]. However, this problem has been solved through the development and implementation of different techniques in common battery management systems. Another problem arises when a series of cells in a battery pack becomes imbalanced, according to Z. B. Omariba, L. Zhang, and D. Sun the imbalance may lead to increased losses and or heating effects, reduced charge, low energy efficiency, and accelerated degradation [9].

Recently, various authors and researchers have been developing different methods and circuits capable of achieving this purpose. In the overview of the latest balancing technologies [1], it can be observed that various cell balancing algorithms have been established for Li-ion batteries. These techniques are categorized as passive and active cell balancing methods. One of the active methods is called 'Switching Shunt Resistor' method, where the operation principle allows cells with a higher energy level to discharge through a resistor, depleting the excess of energy as heat [3].

On the other hand, active methos includes Capacitor based methods, where surplus charge from cells, with higher energy level, are released and stored in the capacitors and then transferred to cells with a lower energy level. Y. Ye, et al. claim that the application of the SC-based balancing method offers a relatively straightforward and cost-effective approach for battery management systems [4]. Another investigated active method is known as Inductor and transformer-based techniques. Those methods involve the transfer of unequal energy from cells or cell groups with higher energy levels to cells with lower energy levels or different cell groups. This transfer is facilitated through the utilization of magnetic components, such as inductors or transformers [1].

Y. Zhang and S. Lu [7— developed and implemented a novel charging method that consists of a series-parallel switching charging equalization. The model establishes a two-phase charging method. Phase 1 begins with a const current series charging circuit, ensuring a swift charging of individual cells. In Phase 2, a microcontroller enables parallel constant voltage charging achieving final equalization among the batteries. The proposed series-parallel switching charge equalization circuit offers benefits including energy balance consideration during charging, simplified control, and fast charging speed with expandability. [7]

Further advanced industrial developments have been made by Texas Instruments, called Battery fuel gauges [8] [9]. Battery fuel gauges are integrated circuits (ICs) that offer a wide array of features, including State of Charge (SOC) Measurement, Capacity Estimation, Voltage Monitoring, Current Monitoring, Temperature Monitoring, and Coulomb Counting. The most advanced devices can support up to 15 cells in a series configuration. These ICs are capable of cell balancing while charging or at rest. The cell balancing algorithm prevents fully charged cells from overcharging and causing excessive degradation and prevents premature charge termination [8]. These devices process this balancing by bypassing the current of each cell during charging or rest. However, no ICs were found capable of cell balancing when the batteries are in parallel connection. One notable limitation in development is the absence of balancing control for parallel configurations. This limitation is crucial to avoid the risk of high current flows within cells arising from significant voltage differences and required time to achieve perfect balancing.

Building on the information above, we established the focus of our research to explore parallel battery configurations. Numerous studies have highlighted that when two batteries are connected in parallel, they begin to balance themselves, with the battery possessing the highest voltage actively regulating, while the battery with the lowest voltage assumes a passive role.

4. Objectives

• Design of an integrated system with an independent power source that includes a battery pack capable of diagnosing and correcting the charge states of individual cells: The main objective is to develop a system that allows monitoring and managing the charge status of each cell individually. This will involve implementing sensors and diagnostic algorithms to detect potential imbalances in the charge state and apply appropriate corrections to optimize the performance of the battery pack.

• Design of a circuit capable of isolating individual cells: The aim is to design and develop a circuit that enables the temporary isolation of each cell individually, thereby facilitating precise modification of its charge state. This isolation capability will allow leveling and balancing the charge state of each cell, thereby improving the overall performance and efficiency of the battery pack.

• Design of a battery charging and discharging system: The goal is to develop a charge and discharge management system that charges two battery cells separately to avoid energy loss. This involves designing a controlled charge/discharge circuit and implementing algorithms that enable precise energy flow management, avoiding overcharging or deep discharges that may affect the battery's lifespan and performance.

5. State of art

5.1 Switching shunt resistor method

Passive cell balancing stands out as a more straightforward and cost-effective balancing approach, widely employed compared to active cell balancing techniques. This strategy operates on the principle of allowing cells with higher energy levels to discharge through passive electronic elements, like resistors, dissipating the excess energy as heat until equilibrium is achieved with cells holding lower energy levels. The major drawback of passive cell balancing is energy is not distributed across the cells in battery pack rather it's being wasted in the form of heat [3].

Utilizing a switched shunt resistor arrangement, passive cell balancing involves the incorporation of resistors linked in parallel with individual cells. These resistors are regulated based on various parameters including State of Charge (SOC), State of Health (SOH), terminal voltage of cells, and available power. The quantity of balancing circuits necessary aligns with the overall count of cells within the battery pack. Specifically, for a battery pack comprising 'n' cells, an equivalent number of 'n' balancing circuits are requisite [3].

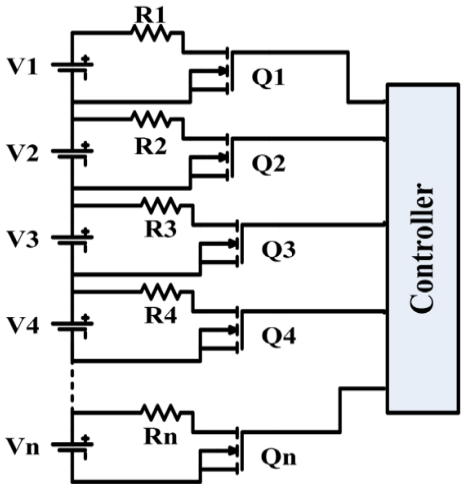

Figure 1. Switching shunt resistor cell balancing circuit [1]

5.2 Capacitor based active balancing method

This approach is referred to as the charge shuttling method, where surplus charge from cells with higher energy levels is first released and stored in capacitors before being transferred to cells with lower energy levels. This method can be categorized

into two types: employing either a single capacitor or multiple capacitors for equalization purposes.

The fundamental concept of this circuit involves achieving charge equilibrium among individual cells through the charge or discharge process of a shared balancer, often in the form of a capacitor. This component facilitates the transfer of energy between any two cells within a battery string [1].

The cell equalizing approach using multiple capacitors involves transferring charge between adjacent cells. This method falls under the category of switched capacitor methods, and it also includes a variation known as the double-tiered switched capacitor method [1].

Within the switched capacitor method, the mechanism consists of connecting one switched capacitor between each pair of neighboring cells using corresponding semiconductor switches. This setup facilitates the exchange of charge, allowing the transfer from a cell with a higher charge to one with a lower charge [1].

Hence, the application of the SC-based balancing method offers a relatively straightforward and cost-effective approach for battery management systems [4].

The foundational SC-based cell balancing units are delineated in Figure 2. Specifically, Figure 1(a) illustrates the core unit containing ideal components. Incorporating the influence of parasitic resistance (R), representing the cumulative effective equivalent resistance of components, leads to the adaptation of the basic cell balancing unit, as demonstrated in Figure 1(b). Furthermore, Figure 1(c) illustrates the circuit configuration incorporating both R and the complete effective equivalent inductance (L). [4]

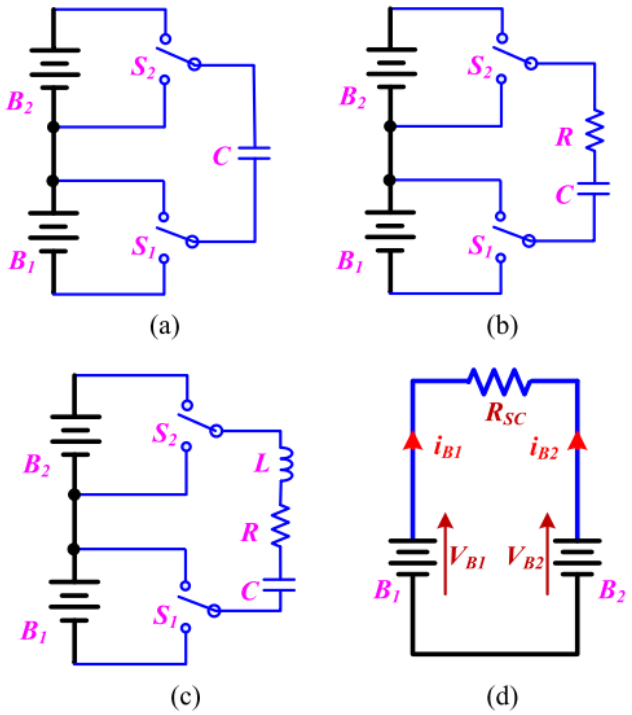

Figure 2. Basic SC-based cell balancing units[4]

5.3 Inductor and transformer based active balancing method

This method is recognized as the energy conversion technique, involving the transfer of unequal energy from cells or cell groups with higher energy levels to cells with lower energy levels or different cell groups. This transfer is facilitated through the utilization of magnetic components, such as inductors or transformers [1].

In this circuit, the fundamental principle is to equalize the charge across each cell through the charge or discharge facilitated by a common balancer, often an inductor. This inductor enables energy transfer between any two cells within a battery string, allowing for seamless energy movement across the battery pack [1].

This technique is often referred to as the direct cell-to-cell method [1]. It distinguishes itself for its simplicity, employing only one inductor to balance the entire battery pack. Notably, it achieves faster balancing speeds compared to capacitor-based topologies and boasts higher efficiency [1]. However, its implementation comes with elevated costs due to the need for numerous semiconductor switches and advanced control techniques to manage these switches.

The configuration of the cell equalizing circuit using several inductors is depicted in Figure 3. In this approach, an inductor is connected between two adjacent cells. The controller monitors the voltage difference between these cells and orchestrates the energy transfer from a higher-charged cell to achieve balance.

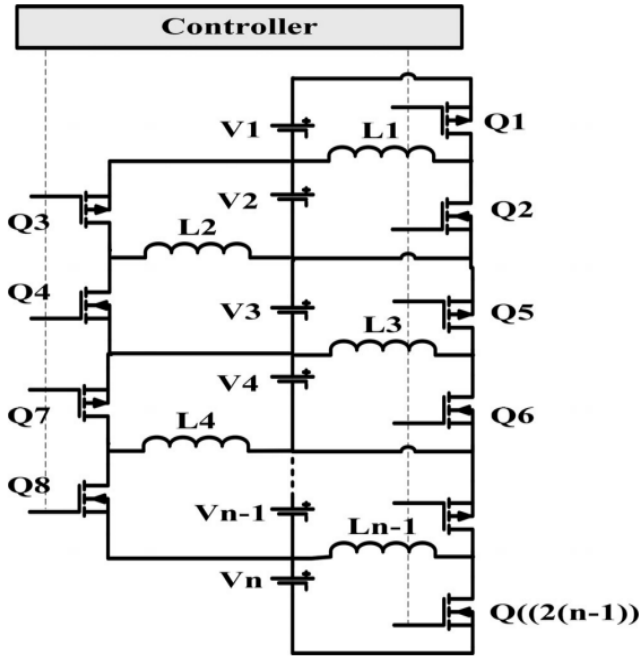

Figure 3. Several inductors based cell equalizing circuit [1]

5.4 Transformer based active balancing schemes

The single transformer balancing method employs the same switching topology as the single capacitor balancing approach [1]. This particular balancing circuit necessitates the use of n + 5 semiconductor switches and just one transformer to achieve balance among the charge levels of n cells.

The foundational principle of this balancing circuit revolves around the utilization of both the "pack to cell" technique and the "cell to pack" technique [1]. In the "pack to cell" approach, the complete battery pack current is directed (via S1) into the transformer T, and the transformed output is rectified and directed to the cell with the lowest charge level through associated semiconductor switches. As a result, controlled operations are crucial to select a target cell and manage switching devices [1].

Conversely, in the "cell to pack" technique, the target cell is a cell with higher energy content, and it's integrated into the battery pack through a transformer. This

integration ensures the voltage of the target cell aligns with that of the other cells within the battery pack, thereby achieving balance [1].

5.5 BUCK-BOOST Strategy (parallel battery cells)

Even among parallel-connected battery cells, an energy imbalance can arise, necessitating a careful examination of this issue across the cells. To address this M. O. Qays, et al. in [5] developed an innovative approach employing a Backpropagation Neural Network (BPNN) methodology to formulate a Battery Management System (BMS). This system adeptly assesses the charging status of individual cells and orchestrates its functions using a DC/DC Buck-Boost converter. Simulation results affirm the effectiveness of this approach in achieving energy equilibrium among parallel-connected battery cells. Impressively, the state of charge (SOC) estimation error is remarkably low, measuring at just 1.15%.

In order to standardize energy transfer among cell sequences, the DC/DC converter incorporates four MOSFET switches (M1~M4). This converter can function as a Buck, Boost, or Buck-Boost converter, adapting its mode based on the expected cell voltage. When operating in Buck mode, M3 remains off while M4 is turned on, with M1 and M2 being governed by a prescribed formula. As depicted in Figure #, the source power initiates the inductor charging and discharging cycles by alternately opening and closing the MOSFET switches M1 and M2. During the charging phase, the capacitor disburses the output current, while the discharging phase is governed by closing and opening M2 and M1 respectively. For loading purposes, the reserved energy from the inductor is supplied to the capacitor. By adjusting the duty cycle (D) to be less than 1, an average terminal voltage (VTer = DVSC) is achieved. Conversely, during Boost mode, M1 and M2 remain on and off respectively, while M3 and M4 are consistently opened and closed to follow the inductor's charging status. This sequence is reversed during the discharging period. [5]

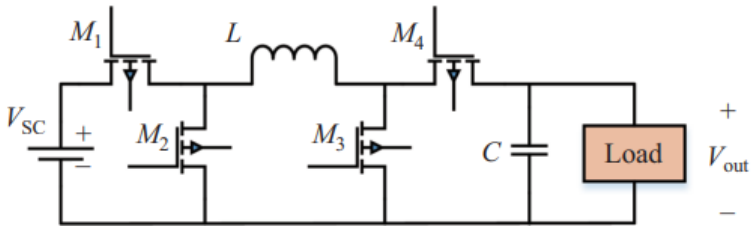

Figure 4. Four switched DC/DC Buck-Boost converter [5]

Figure 4. Four switched DC/DC Buck-Boost converter

To mitigate SoC discrepancies among cells, an active cell balancing method is introduced. The Battery Management System (BMS) gauges SoC for each cell,

emitting a balancing directive via the DC/DC synchronous Buck-Boost converter (depicted in Figure 4). In this approach, the average SoC ($\bar{S}$) of parallel-connected cells is juxtaposed against individual cell SoCs (Si) [5]. When the variation surpasses or falls below a predefined threshold (Sthr), the BMS directs the converter accordingly:

$$\begin{cases} S_i - \bar{S} > S_{\text{thr}} & \text{Discharging} \\ S_i - \bar{S} < S_{\text{thr}} & \text{Charging} \\ \text{Others} & \text{Islanding} \end{cases}$$

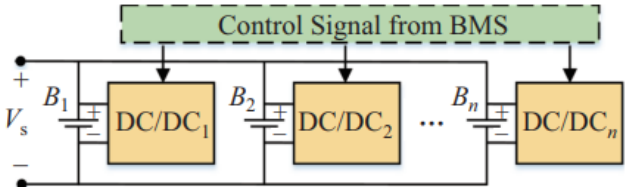

Figure 5. Expanded circuit diagram [5]

5.6 Constant temperature – constant voltage charging method using PID controller.

Overvoltage and overheating are critical factors that negatively impact the battery's lifespan. To combat these issues, an advanced battery management system (BMS) can be implemented. The BMS incorporates a PID (Proportional-Integral-Derivative) controller to regulate the charging current effectively.

A thermal model of the battery is proposed, it is essential for predicting and managing temperature changes during charging and discharging cycles. A well-constructed thermal model enables the close loop system to anticipate temperature fluctuations and apply appropriate control strategies to maintain optimal operating conditions. Rise in surface temperature (Ts) and internal temperature (Ti) of the battery causes the power loss (PL). The thermal model is shown in the figure below.

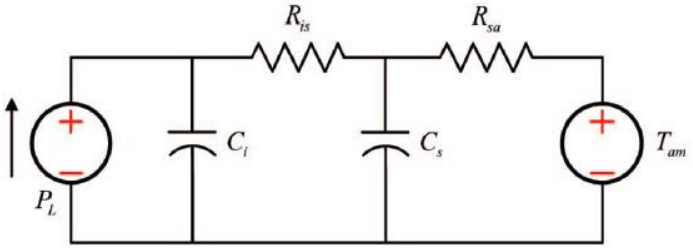

Figure 6. Thermal circuit model [6]

Figure 6. Thermal circuit model

Where Ci is internal heat capacity, T is the battery temperature, Ris is internal to surface thermal resistance, Cs is surface heat capacity, Tam is ambient temperature, Rsa is surface to ambient thermal resistance. [6]

The PID controller continuously monitors the battery temperature and adjusts the charging current to regulate the temperature below the limit. Monitoring battery temperature is crucial for preventing overheating and ensuring safe operation. The BMS incorporates temperature sensors distributed across the battery pack to collect real-time temperature data. This data is then compared to a reference temperature, which is the maximum temperature allowed by the battery cell. If the measured temperature exceeds this threshold, the BMS can take corrective actions, such as reducing the charging current. Close loop block diagram below.

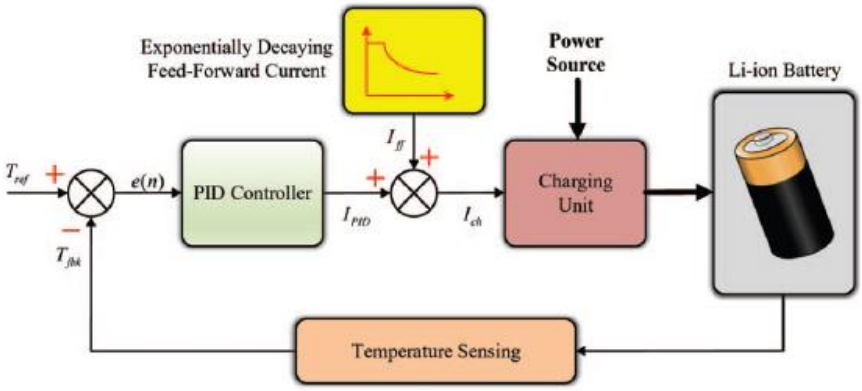

Figure 7. Control loop block diagram [6]

The CTCV charging technique is an innovative approach to enhance charging efficiency while maintaining battery health. Unlike the constant current constant voltage (CCCV) technique, where the current remains constant until the voltage reaches the set level, the CTCV method adjusts the charging current to maintain a constant battery temperature while the voltage increases. This technique has been shown to reduce charging time by approximately 24% compared to the CCCV approach. By controlling temperature and voltage simultaneously, the CTCV technique minimizes the risk of overheating and overcharging.

5.7 Series-Parallel Connection Switching Charging Method

[7] The paper addresses the issue of unbalanced charging in power lithium battery packs, which hampers efficient energy utilization in autonomous underwater vehicles (AUVs). To tackle this problem, a novel charging method is introduced. A series-parallel switching charging equalization method is proposed, supported by a designed circuit, and explained working principles. A corresponding model is

established, and simulation experiments are conducted. Results indicate that the proposed method mitigates charging current impact and significantly enhances battery cell charging balance.

To analyze battery behavior, The following Thevenin equivalent circuit is proposed. This model simplifies the battery's complex behavior into a more manageable representation, comprising a voltage source in series with an internal resistance. This approach aids in understanding and predicting battery responses during various charging and discharging scenarios.

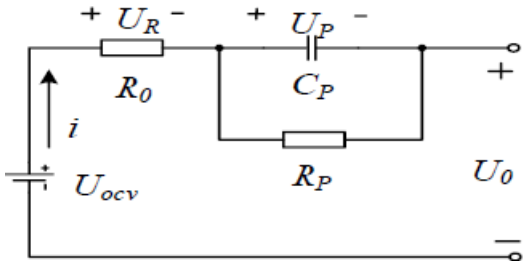

Figure 8. Charging method circuit [7]

In the proposed two-phase charging method, Phase 1 involves initiating a constant current series charging circuit for the battery pack. This arrangement ensures swift charging of individual cells. In Phase 2, during the charging process, the microcontroller enables parallel constant voltage charging. As per GB/T18287-2000 standards, the battery pack is considered fully charged when the detected charging current drops below 0.01C, where C represents the rated capacity of a single cell. The proposed series-parallel switching charge equalization circuit offers benefits including energy balance consideration during charging, simplified control, and fast charging speed with expandability.

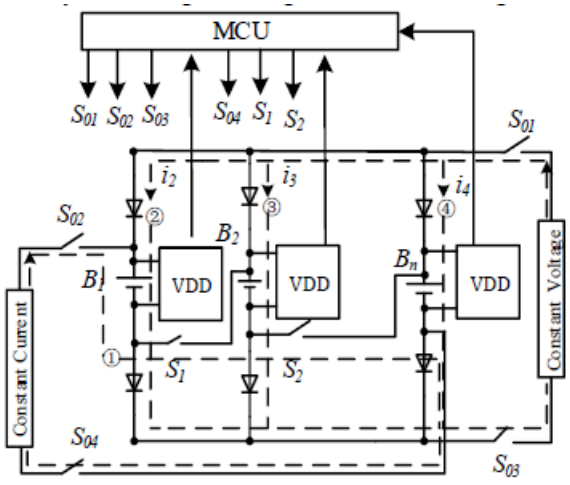

Figure 9. Switching charging method functional diagram [7]

5.8 Battery fuel gauges

Battery fuel gauges are integrated circuits (ICs) that offer a wide array of features, including State of Charge (SOC) Measurement, Capacity Estimation, Voltage Monitoring, Current Monitoring, Temperature Monitoring, and Coulomb Counting. The most advanced devices can support up to 15 cells in a series configuration.

Building on the information above, we established the focus of our research to explore parallel battery configurations. Numerous studies have highlighted that when two batteries are connected in parallel, they begin to balance themselves, with the battery possessing the highest voltage actively regulating, while the battery with the lowest voltage assumes a passive role.

6. Methodology

6.1 Initial tests

Initially, we conducted tests by connecting two unbalanced cells in parallel and measuring the open circuit voltage (OCV) and current during the first hour after the connection. In other words, we took measurements more frequently at the beginning and less frequently as time passed. It is important to note that the power transferred from one battery to another is directly proportional to the voltage difference between the batteries. In simpler terms, the greater the voltage difference, the faster the battery with the higher voltage discharges energy to the battery with the lower voltage.

Time (min)	BAT 1 (V)	BAT 7 (V)	Current (A)	Delta (V)	Sum (V)
0	3.091	3.994	0.327	0.903	7.085
1	3.304	3.982	0.261	0.678	7.286
2	3.35	3.98	0.251	0.63	7.33
5	3.486	3.969	0.202	0.483	7.455
9	3.577	3.957	0.162	0.38	7.534
15	3.651	3.941	0.118	0.29	7.592
23	3.705	3.925	0.086	0.22	7.63
29	3.721	3.925	0.053	0.204	7.646
39	3.75	3.915	0.051	0.165	7.665

Table 1. Batteries 1 and 7 voltage and current when balancing in parallel.

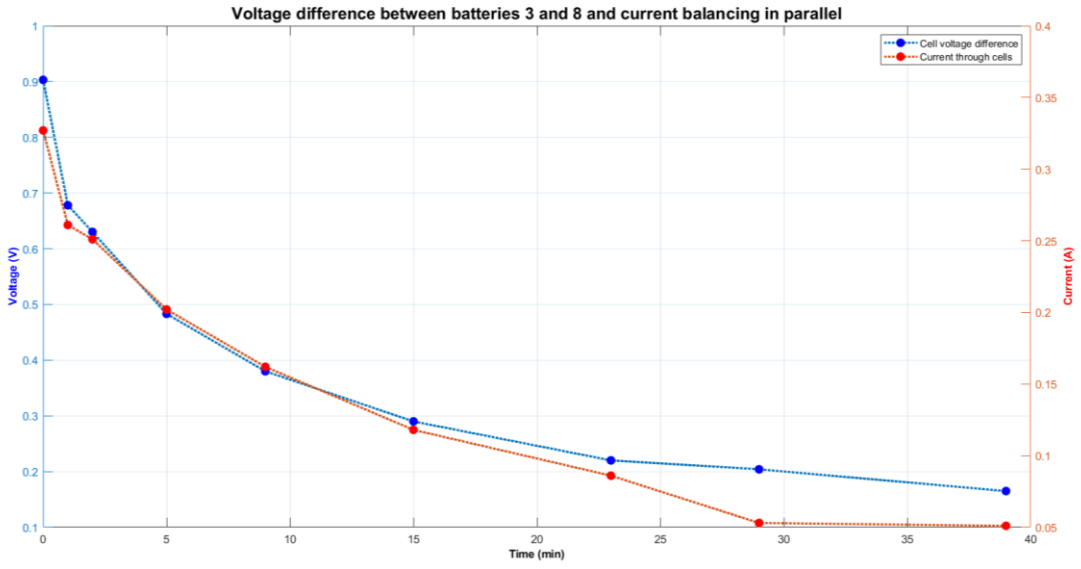

Figure 10. Voltage difference between batteries 3 and 8 and current when balancing in parallel.

The results confirmed that the battery with the highest voltage indeed transferred energy to the battery with the lowest voltage, with current decreasing over time. However, it became evident that it takes more than an hour for the batteries to achieve perfect balance. This prompted us to conduct another test to ascertain that the batteries could eventually reach a state of perfect balance.

Time (min)	BAT 3 (V)	BAT 8 (V)	Delta (V)
0	3.775	3.453	0.322
1	3.757	3.541	0.216
2	3.747	3.6	0.147
3	3.744	3.628	0.116
4	3.741	3.645	0.096
5	3.74	3.653	0.087
10	3.748	3.646	0.102
1211	3.738	3.738	0

Table 2. Batteries 3 and 8 voltage and when balancing in parallel: 3 Dominant.

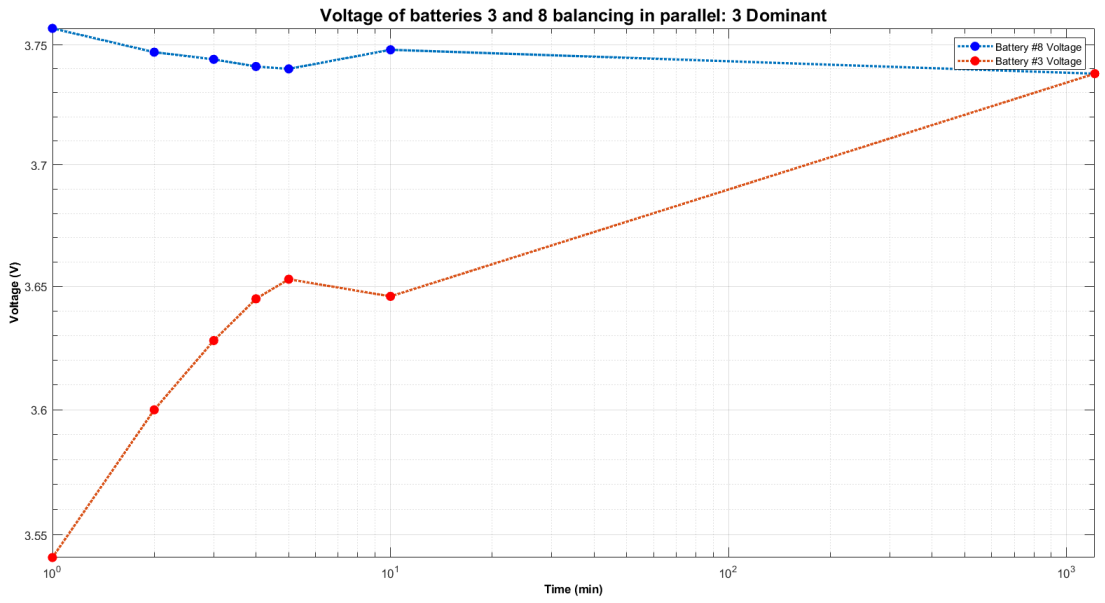

Figure 11. Voltage of batteries 3 and 8 balancing in parallel: 3 Dominant.

The test results indicated that the batteries effectively balanced themselves after 1211 hours of being connected. In other words, the battery cells achieved a full balance at or before the 1211-hour mark. To further validate the balancing mechanism of battery cells connected in parallel, with the highest voltage cell acting as the active source and the lowest voltage cell as the passive element, we

conducted a test where we reversed the roles of the previously identified battery cells.

Time (min)	BAT 3 (V)	BAT 8 (V)	Delta (V)	Sum (V)
0	3.456	3.985	0.529	7.441
1	3.592	3.926	0.334	7.518
2	3.616	3.916	0.3	7.532
4	3.683	3.881	0.198	7.564
6	3.72	3.872	0.152	7.592
9	3.749	3.872	0.123	7.621
13	3.779	3.87	0.091	7.649
18	3.791	3.867	0.076	7.658
22	3.795	3.866	0.071	7.661
30	3.797	3.864	0.067	7.661
37	3.808	3.858	0.05	7.666
48	3.815	3.854	0.039	7.669
60	3.823	3.851	0.028	7.674

Table 3. Batteries 3 and 8 voltage and when balancing in parallel: 8 Dominant.

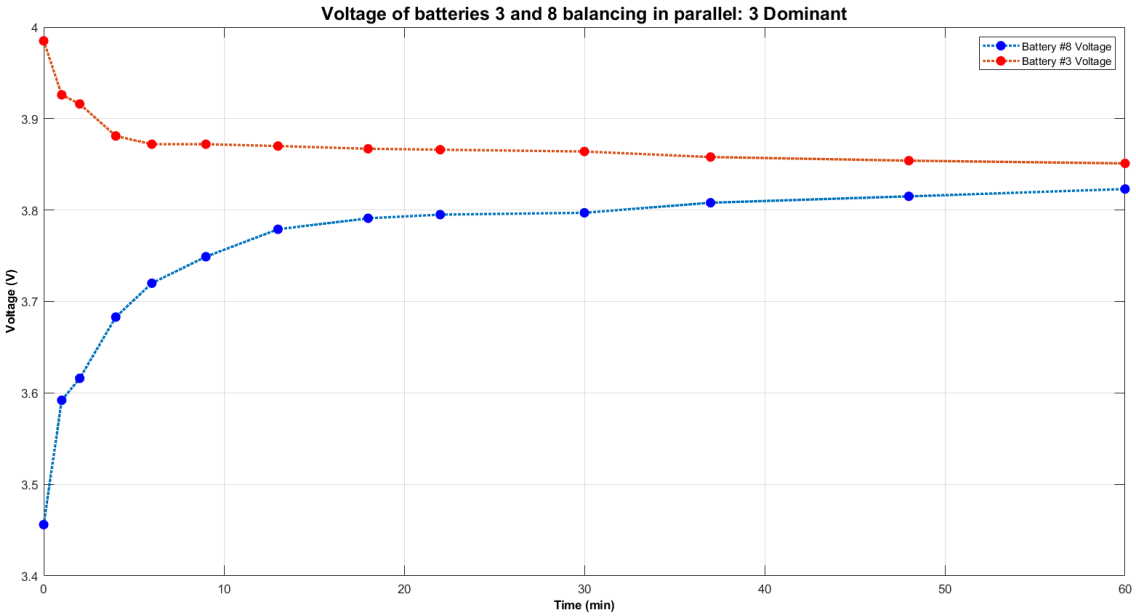

Figure 12. Voltage of batteries 3 and 8 balancing in parallel: 8 Dominant.

Once again, the results confirmed that the battery with the highest voltage supplied energy to the battery with the lowest voltage, regardless of the specific battery cell involved in the process.

6.2 Circuit design

For schematic design and PCB consolidation, Altium Designer software was used. When connected to the net, the circuit is powered by an AC-DC power supply with a type-C USB adaptor as presented in figure 13.

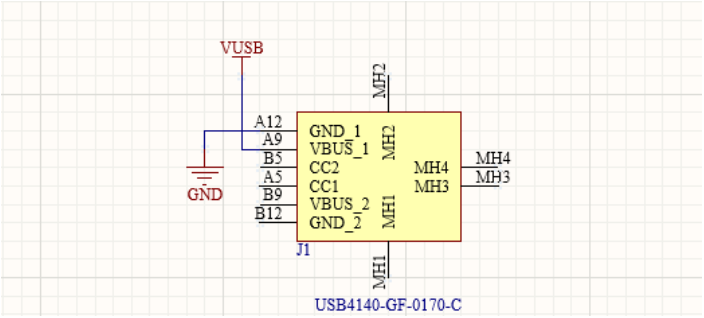

Figure 13. Type-C USB module connections.

In figure 14 the microprocessor (IC1) is shown, it accomplishes the following functions:

Inputs: Voltage read through RA0 and RA1 ADCs.

Outputs: I2C communication to OLED display through RC3 and RC4.

UART communication through RC6 and RC7.

Relays activation through RB0, RB1 and RB2.

Battery management ICs enabler through RB3 and RB4.

Functioning test circuit through RA2 and RC0.

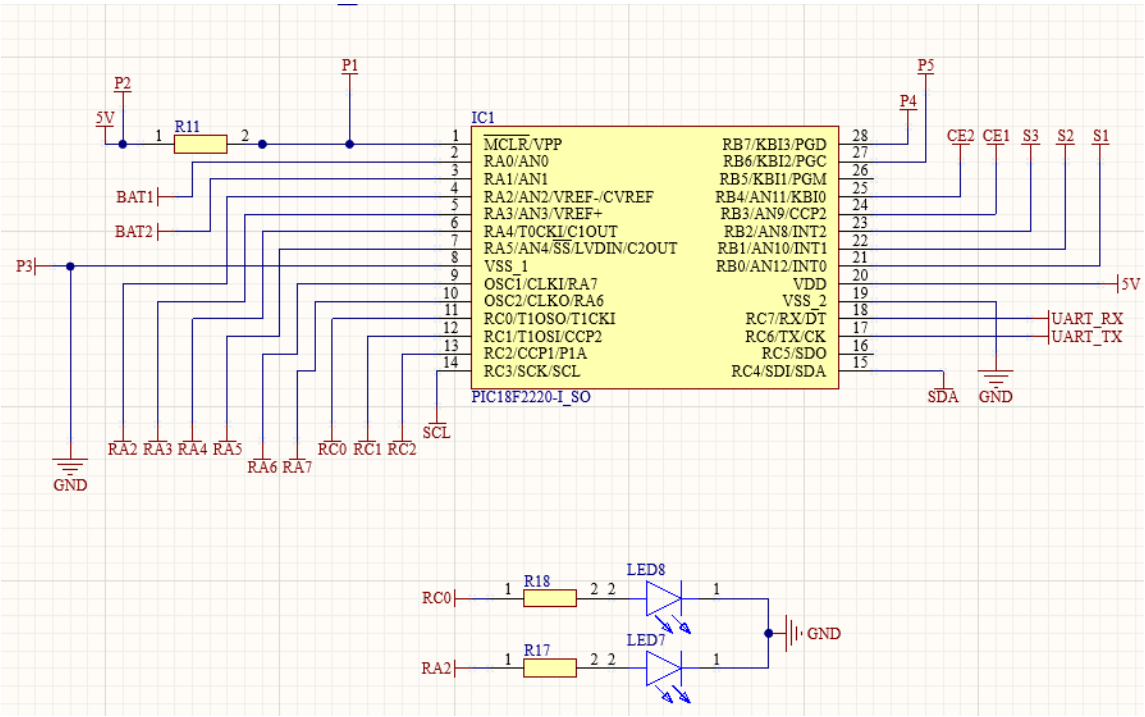

Figure 14. Microprocessor PIC18F2220 connections.

In figure 15 Battery management ICs (BT1, BT2) are presented, each IC provides with charge/discharge capabilities for one single battery cell. Resistor calculations are listed below.

The MCP73871T allows constant current mode (*Ireg*) control by implementing a resistor on pin PROG1, using following formula:

$$Rprog1 = \frac{1000\ V}{Ireg} = \frac{1000\ V}{454\ mA} = 2.2\ K\Omega\ \ (I)$$

Similarly, the charge termination current threshold (*Itermination*) can be adjusted by implementing a resistor on pin PROG3, a current equal to approximately 10% of charge current was selected.

$$Rprog3 = \frac{1000\ V}{Itermination} = \frac{1000\ V}{30.3\ mA} = 33\ K\Omega\ \ (II)$$

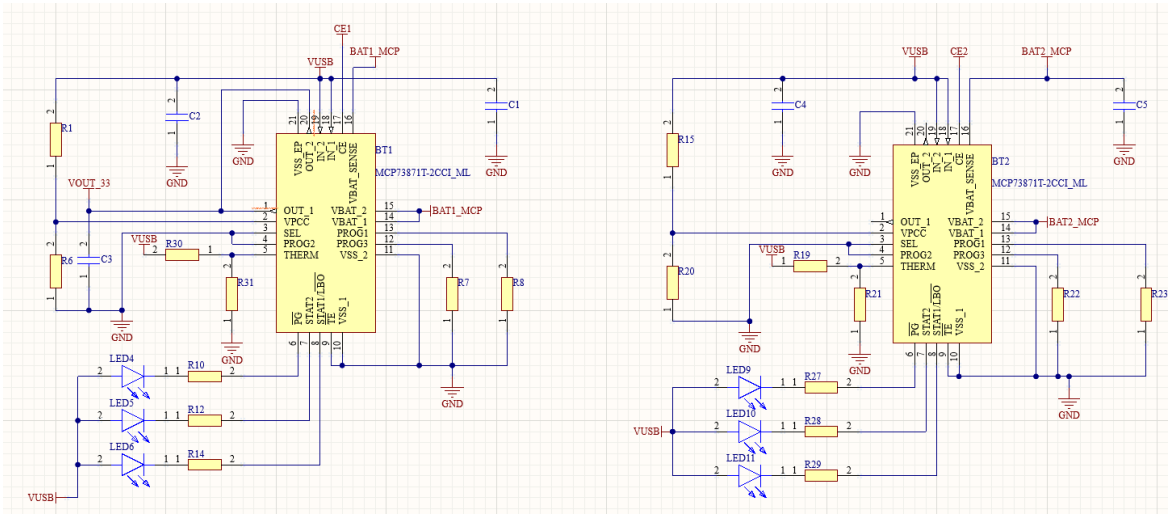

Figure 15. Battery management ICs MCP73871T connections.

Please note that other passive components present in the circuit were selected according to the manufacturer recommendation available on the Datasheet.

Many possible applications might need a constant voltage supply of 5V, for this reason a DC-DC Boost converter (IC2) was implemented as shown in figure 16.

The TPS61027DRCR allows to set a maximum voltage limit by selecting *R16* and *R24* according to the following formula:

$$R16 = R24 * \left(\frac{Vo}{VFB} - 1\right) \quad (III)$$

Where *Vo* is the output voltage and *VFB* the typical voltage of the FB pin which is 500mV. Furthermore, the value of *R24* cannot exceed $500\,K\Omega$ and must be in the range of $200\,K\Omega$. To ensure $R24 = 200\,K\Omega$ and $Vo = 5V$, $R16 = 1.8\,M\Omega$ was selected.

Additionally, the minimum battery voltage ($Vbat\_min$) can be adjusted by selecting *R25* and *R26* according to the following formula:

$$R25 = R26 * \left(\frac{Vbat\_min}{Vlbi - thereshold} - 1\right) \quad (IV)$$

Where $Vlbi - thereshold$ is LBI voltage generated on-chip. Furthermore, the value of *R26* must be in the range of $500\,K\Omega$. To ensure $R26 = 390\,K\Omega$ and $Vbat\_min = 2.81\,V$, $R25 = 1.8\,M\Omega$ was selected.

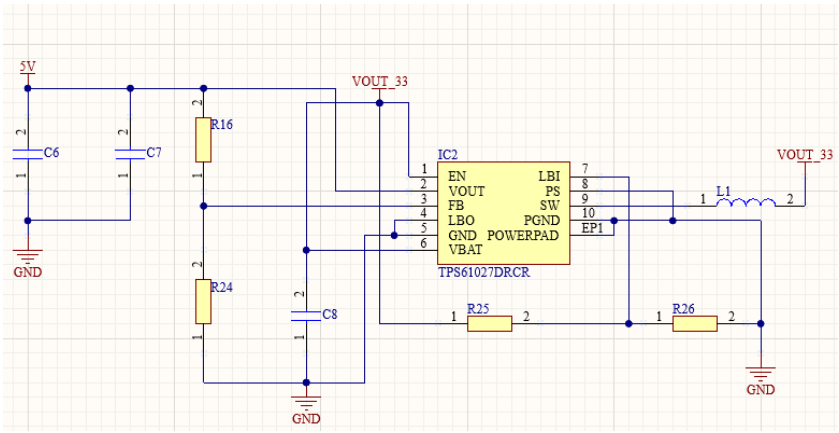

Figure 16. DC-DC Boost converter connections.

Please note that other passive components present in the circuit were selected according to the manufacturer recommendation available on the Datasheet.

For switching the batteries and the battery management ICs, the relays (K1, K2, K3) presented in figure 17 were implemented and have the following functioning logic:

- K1 switches the connection of battery 1 between BT1 and the microprocessor analog input for OCV measurement.

- K2 switches the connection of battery 2 between BT2 and K3 COM_1 pin and K3 switches the connection of K2 NO pin and between the microprocessor analog input for OCV measurement.

Building on the above, when battery 2 ends charging K2 switches to K3 and K3 switches either to a voltage measurement or a parallel connection with battery 1, which is ensured only when both battery cells are balanced.

The switching is controlled by the microprocessor (S1, S2, S3) through a transistor to ensure the activation current of the relays.

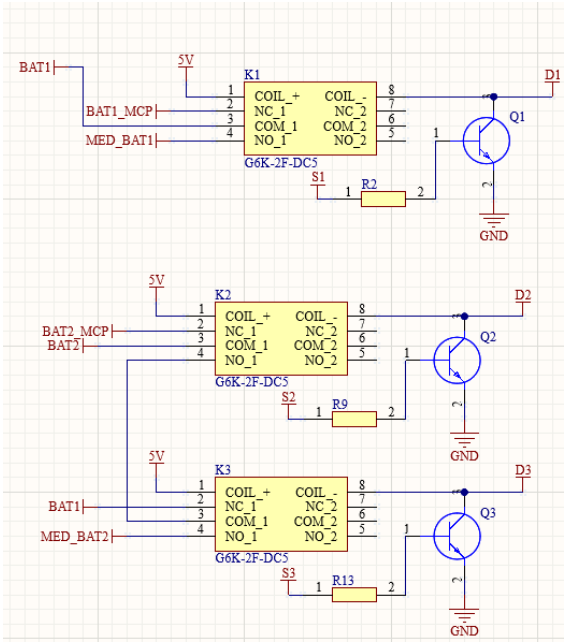

Figure 17. Relays connections

6.3 Programing workflow

6.3.1 Workflow 1

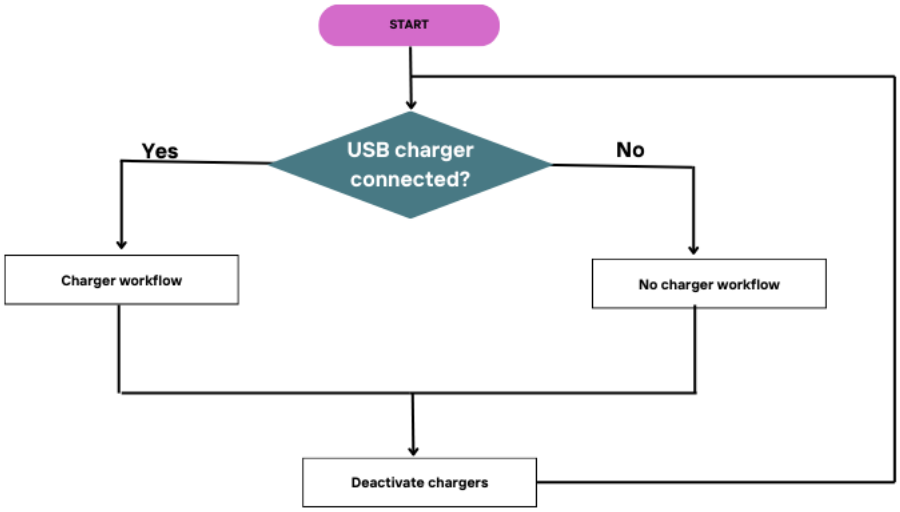

Figure 18. USB Workflow.

The first part of the program consists of measuring the power input of the charging circuit. Whether it is connected or not, the program will run either the charger workflow or the no-charger workflow. At the end of either workflow, the integrated circuits chargers are disabled to avoid unpredictable charging. This could potentially occur if USB power is connected during a transitory state of the program.

The circuit was designed to prevent auto cell balancing when the batteries are connected, and the circuit is powered off. This was addressed by leaving the switch that isolates each battery normally open. Therefore, to supply a charge to the two batteries, the circuit needs to be powered on.

6.3.2 Charger workflow

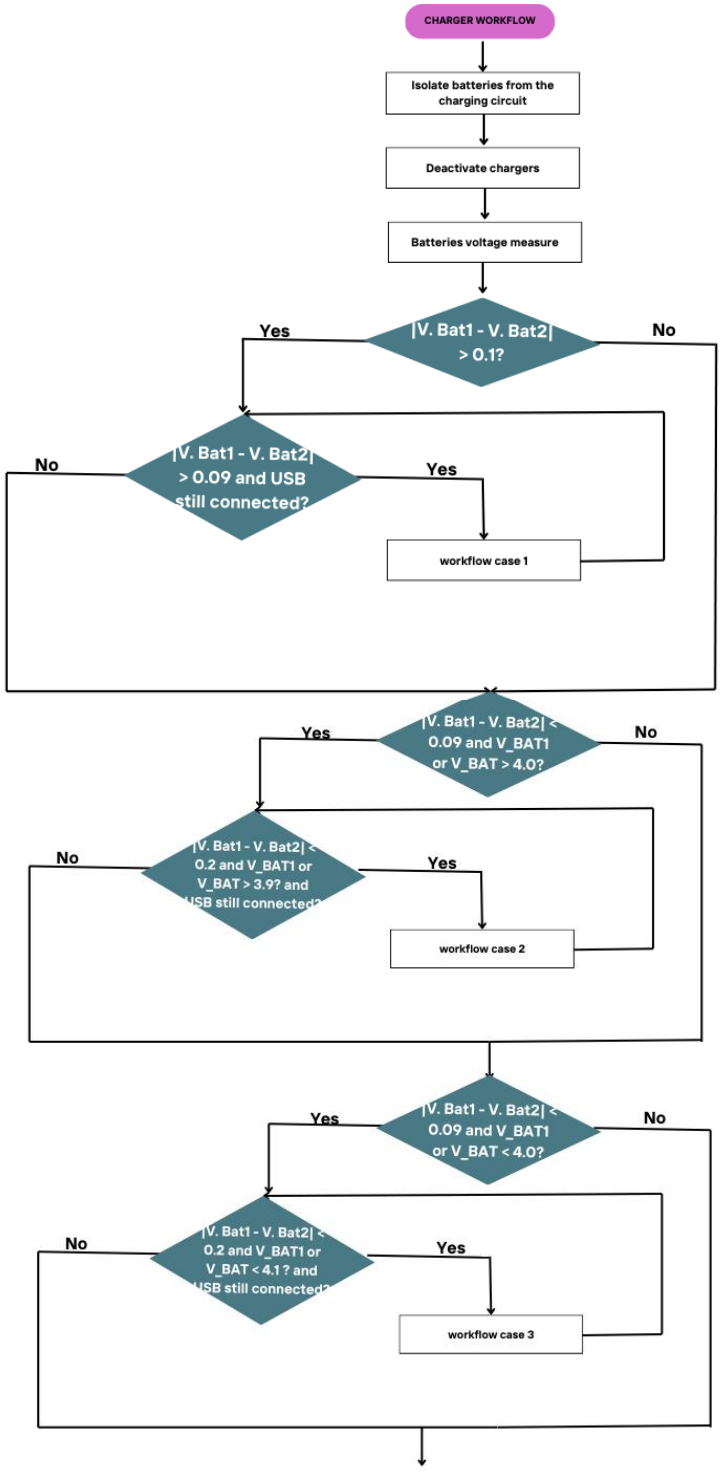

Figure 19. Charger workflow

If the USB power is plugged in, the charging workflow is initiated. In this scenario, there are three cases. The first case is applicable when the batteries have a voltage difference of more than 0.1 V between each other. The second possibility is triggered when the batteries have a disbalance of less than 0.1 V, but one battery needs to be over 4.0 V. This indicates that both batteries have a sufficient level of charge and can be connected in parallel for automatic balancing without the need for any algorithms. In the last case, the batteries don't have more than a 0.1 V difference. However, since they have less than 4.0 V, they can still be charged together.

In each case, there is an initial conditional statement that checks for voltage difference and/or a voltage value from each battery. After the first conditional is validated, there is a second conditional within a while loop, where the values are slightly adjusted. For instance, in case number 2, if the voltage difference is 0.09, then it must exceed 0.2 to exit the loop. Additionally, if the dominant battery voltage is over 4.0 V within the loop, it must be under 3.9 V. This adjustment is made to prevent hysteresis between cases 1, 2, and 3. Otherwise, it might lead to continuous activation and deactivation of the charge, as well as the opening and closing of the parallel connection.

6.3.3 No charger workflow

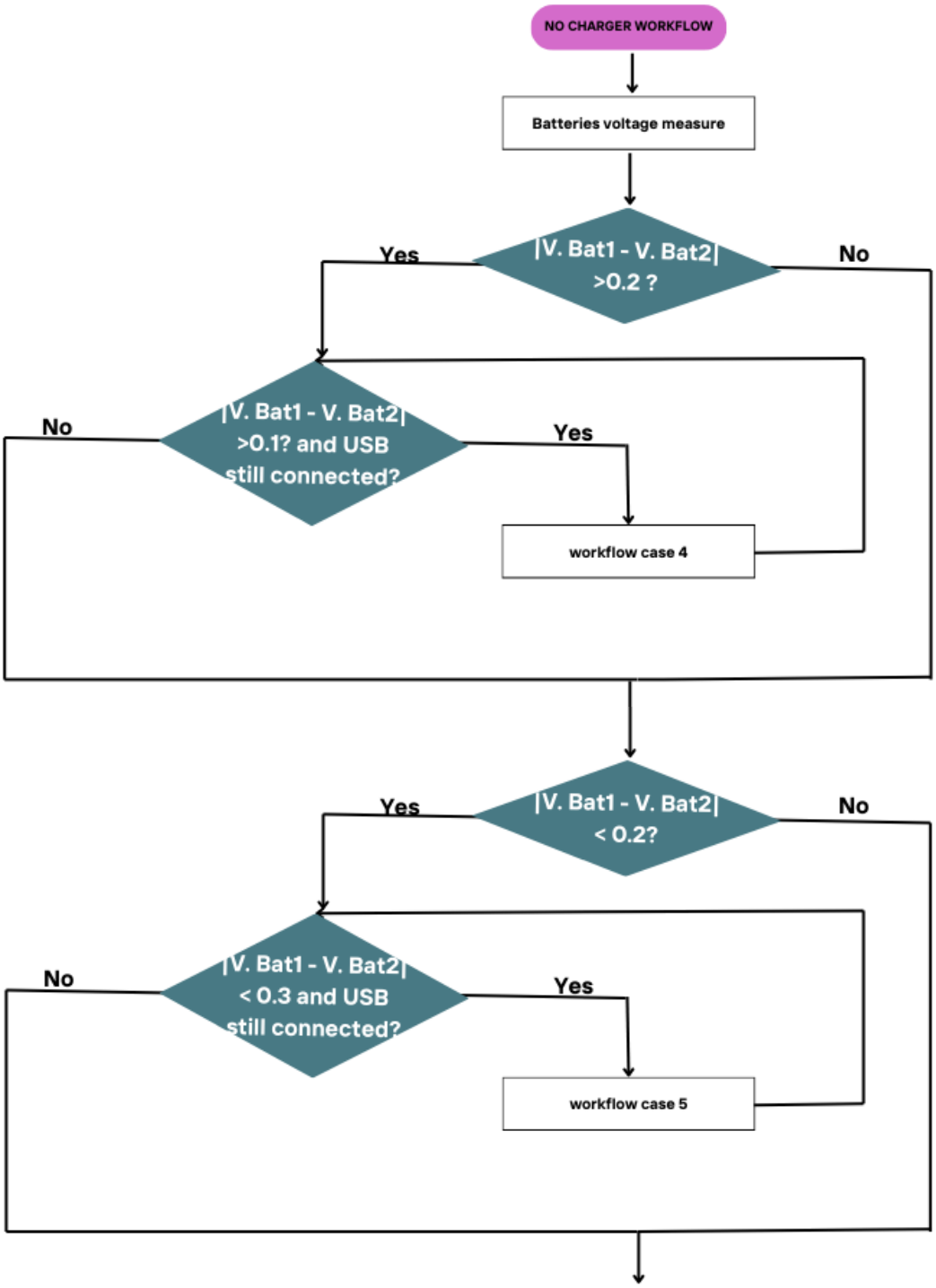

Figure 20. No charger workflow

On the other hand, the previous figure shows the no charging algorithm. Indeed, there are two possible cases. Case 4 is applicable when the batteries have a voltage difference of more than 0.2. Furthermore, case 5 is used when the difference is less than or equal to 0.2. The same logic is applied to both cases, adjusting the difference value between batteries to prevent hysteresis.

6.3.4 Workflow case #1

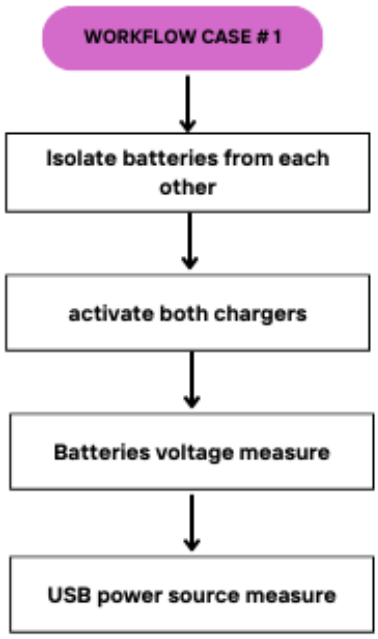

Figure 21. Workflow case #1

In case 1, the batteries are isolated from each other, and each charger is activated. This is done to initiate an independent charge for each battery. The process is maintained until both batteries have a voltage difference of 0.09. In every cycle, the batteries are measured to confirm they are still unbalanced, and the USB power is measured as well to validate that the USB power is still connected.

6.3.5 Workflow case #2

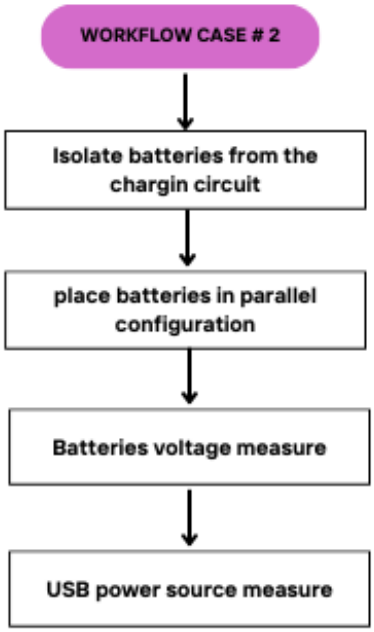

Figure 22. Workflow case #2

Case 2 is the process to balance batteries without the chargers. Batteries are placed in parallel so they can transfer the remaining energy difference between them. Because the voltage variation is small, the batteries won't lose a significant amount of energy. Batteries are isolated from the chargers to avoid any unpredictable circumstances, and once again, the batteries and USB power are measured, on each loop, to confirm that the case is still valid.

6.3.6 Workflow case #3

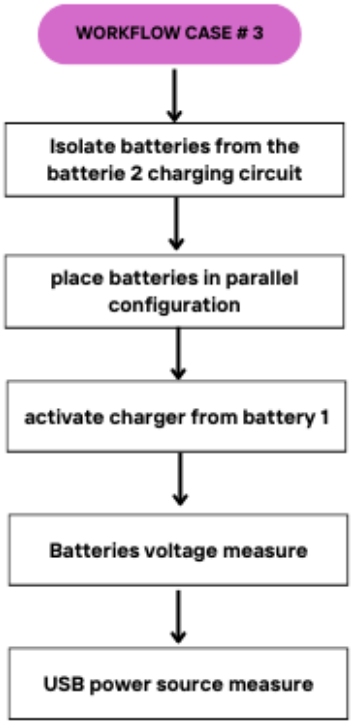

Figure 23. Figure 23. Workflow case #3

In the third scenario, the battery 2 charger is isolated from the batteries by enabling switch 2. Subsequently, the batteries are configured in parallel, and the charger from battery 1 is enabled. This results in a continuous charge to both cells in a balanced condition. The voltage in each battery and USB power is also checked.

6.3.7 Workflow case #4

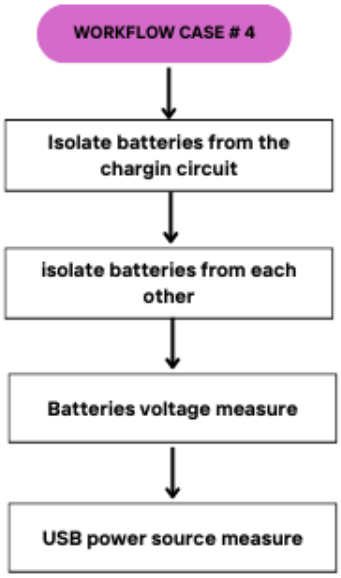

Figure 24. Workflow case #4

Condition 4 is invoked in the absence of USB power. However, as the cells are unbalanced, they are isolated from each other to prevent energy transfer and loss in the process. Furthermore, the circuit shouldn't be prepared to handle any charge, and it is placed in a standby mode, waiting for power to charge and balance the cells. Ultimately, the batteries and USB are validated in every cycle.

6.3.8 Workflow case #5

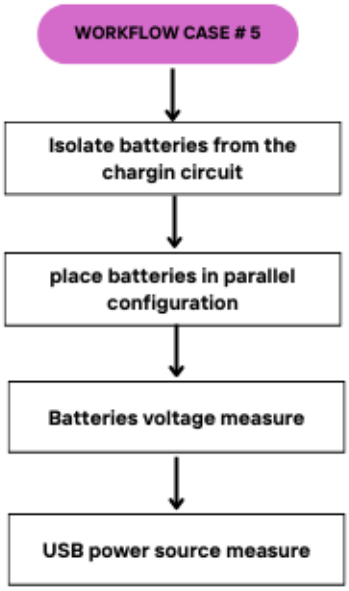

Figure 25. Workflow case #5

In the last option, it is also achieved in a no USB power state. Here, the batteries are almost balanced, and they can be placed in parallel to undergo a natural balance between them. Additionally, this case is ideal for supplying any charge, draining both batteries simultaneously. At the end, battery and USB power measurements are taken.

6.3.9 Interruption

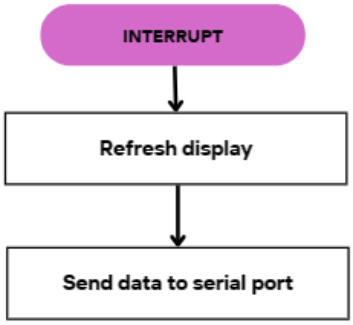

Figure 26. Interruption

An interrupt is configured to send new data to the display in order to provide a visual interface. Furthermore, the data from the ADC measurements is sent through the serial port. This data will be further converted using a TTL to USB adapter and read from a computer. This interrupt is configured to occur every second, resulting in a sampling rate of 1 Hz.

6.4 Calibration

To adjust the ADC output value, calibration was performed using a multimeter from the brand KAL equip, series 3000. The power input to feed the microcontroller was 3.1 V, which served as the reference for the ADC conversion. Voltage measurements were directly taken from the batteries and compared with the ADC value configured for a 3.1 V conversion. However, the error was initially high and was compensated for by dividing the actual measurement by the ADC output. This correction factor was then multiplied by the 3.1 V from the initial reference in the code to reduce the error. It's important to note that each ADC has its own reference value.

$$BAT_1 = \frac{ADC_1}{4095} * 3.3$$

$$BAT_2 = \frac{ADC_1}{4095} * 3.29$$

As shown in Table 4, the calibration results in a low error rate (less than 3%) compared to a measuring device.

BAT #	System (V)	Multimeter(V)	Error
2	3.24	3.17	2%
7	3.26	3.2	2%
3	3.54	3.47	2%
5	3.68	3.59	3%
1	3.77	3.69	2%
9	3.95	3.85	3%

Table 4. Calibration error rate calculation.

6.5 Data log

For the data log, a serial interface was set between the microcontroller and a PC, using Matlab to save and plot the measured data. The programmed code in the microprocessor manages the data log through a function that saves the data taken from the ADC ports and transmits them through the serial port using an UART interface. Considering that there are two series of data being sent (ex. Battery #1

and Battery #2) the printed message initiates with an identifier (1 or 2) to differentiate which port is the data being measured from. Furthermore, the received data is plotted in Matlab simultaneously.

6.6 Component overview

In Table 5 a component overview is listed, for a detailed description please see annexes 10.1.

Component	Reference
LEDs	Different colors
Triple switching diode	BAS116VY-QX
Resistors	Different values
Relays	G6K-2F-DC5
Ceramic Capacitors	Different values
Battery management IC	MCP73871T-2CCI_ML
Microprocessor	PIC18F2220-I_SO
BJT Transistors	SMMBT2222ALT1G
Inductors	SRP3012CC-6R8M
Boost converter	TPS61027DRCR
USB Type C	USB4140-GF-0170-C

Table 5. Component overview

6.7 Devices under test

10 Batteries were used to perform the tests presented in this document; the battery cells share the following specifications:

Devices under test				
Identifier	**Reference**	**Type**	**Manufacturer**	**Capacity**
Battery 1-10	GH 18659	Li-ion	Quilt fire	6800 mAh

7. Results and analysis

7.1 Charge cycle cells unbalanced

Once the designed circuit was implemented, an initial test was conducted. In this test, two unbalanced battery cells were connected to the circuit and voltage measurements were taken through the analog to digital converter of the microcontroller. Results are shown in Figure 27.

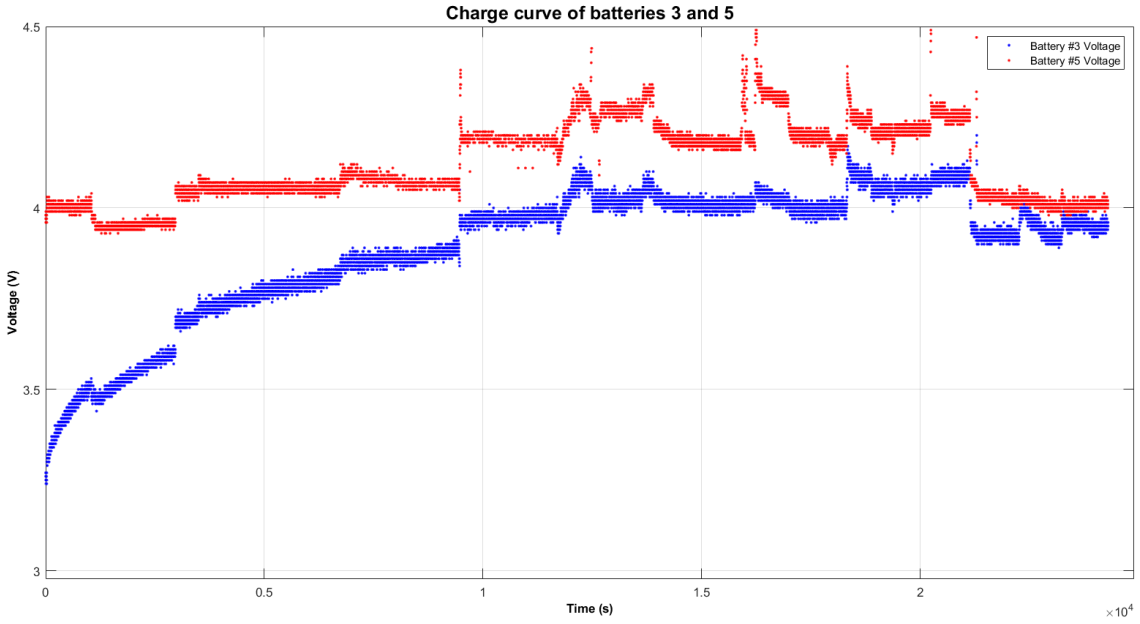

Figure 27. Charge curve of batteries 3 and 5

The presented curve describes two distinct stages. The initial stage spans the first 1.5e4 [s] of the charge cycle, during which the circuit aims to charge both cells to their maximum state of charge (SOC) using one battery charger per cell. As shown in Figure 27, the battery with the lowest voltage (Battery #3(initial) = 3.3[V]) charges faster than the one with the highest voltage (Battery #5(initial) = 3.96[V]). This charging behavior validates earlier test results that showed an exponential reduction in current when the battery cells voltage nears the voltage source. Consequently, the cell voltage increases less as it approaches the voltage source.

The second stage commences when the voltage difference between the two battery cells is higher than the reference in the program Subsequently, the microcontroller activates the relay to connect both battery cells in parallel. This transition occurs at 2.11e4[s], during which both battery voltages become nearly

equal. Calculating the mean voltage of the battery cells within this range (Battery 3 = 3.945[V]; Battery 5 = 4.023[V]), the mean error due to the ADC conversion of the microcontroller is 1.97%.

The curve exhibits minor and major step-ups/step-downs in the measurements, due to the power source supplying the circuit. The microprocessor's analog port data reading and conversion depend on the supply voltage at each measurement instance. Therefore, any increment or decrement in the supply voltage directly affects the measurements. Typically, these supply voltage variations are in the order of mV. However, at certain points, the voltage fluctuations were more significant, resulting in notorious deviations from the mean measurements.

7.2 Discharge cycle

The designed circuit also provides data log for battery cells discharge cycles, the figure 28 shows the discharge curve of batteries 2 and 7, those batteries were connected to a load of (2.2k)

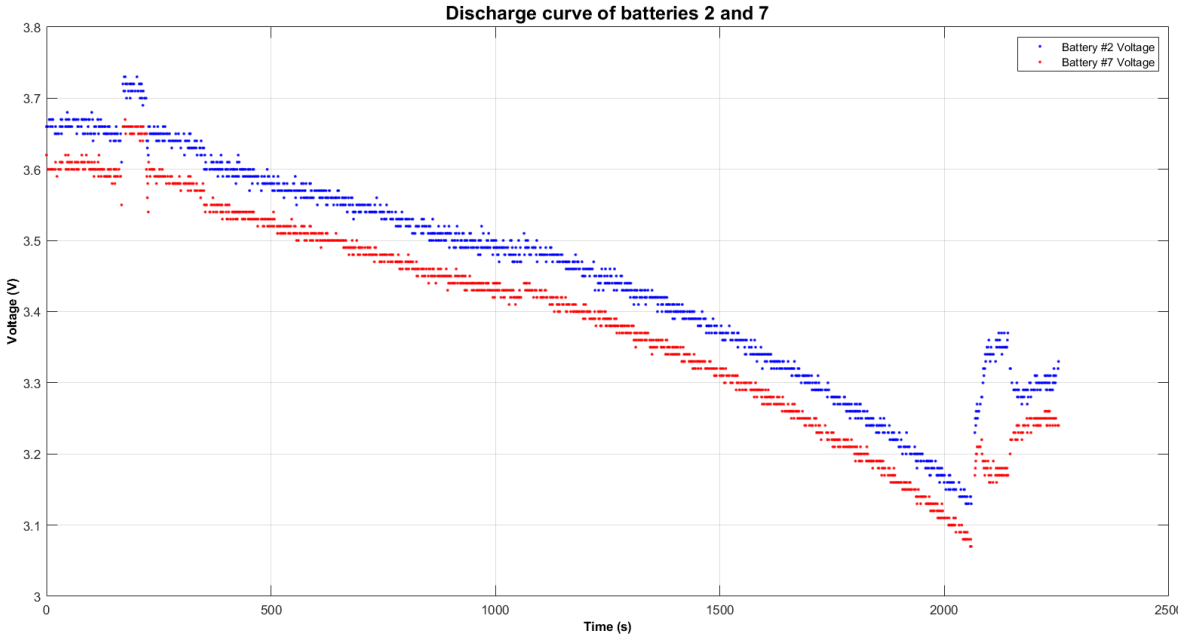

Figure 28. Discharge curve of batteries 2 and 7

Similarly, as presented in Figure 27, an anomaly occurs around 200ms, primarily due to fluctuations in the voltage source. These fluctuations lead to varying readings in the ADC port of the microcontroller. Despite setting both battery cells in parallel, an apparent voltage difference exists between the cells owing to measurement errors and the internal resistance of the relay.

Towards the end of the cycle (at 2100 [s]), the load disconnects from the battery cells, initiating a relaxation period during which the voltage fluctuates before stabilizing.

7.3 Charge cycle cells balanced

Finally, another test was conducted, setting through relays the battery cells 2 and 7 in parallel and charging them with only one battery charger as shown in figure 29.

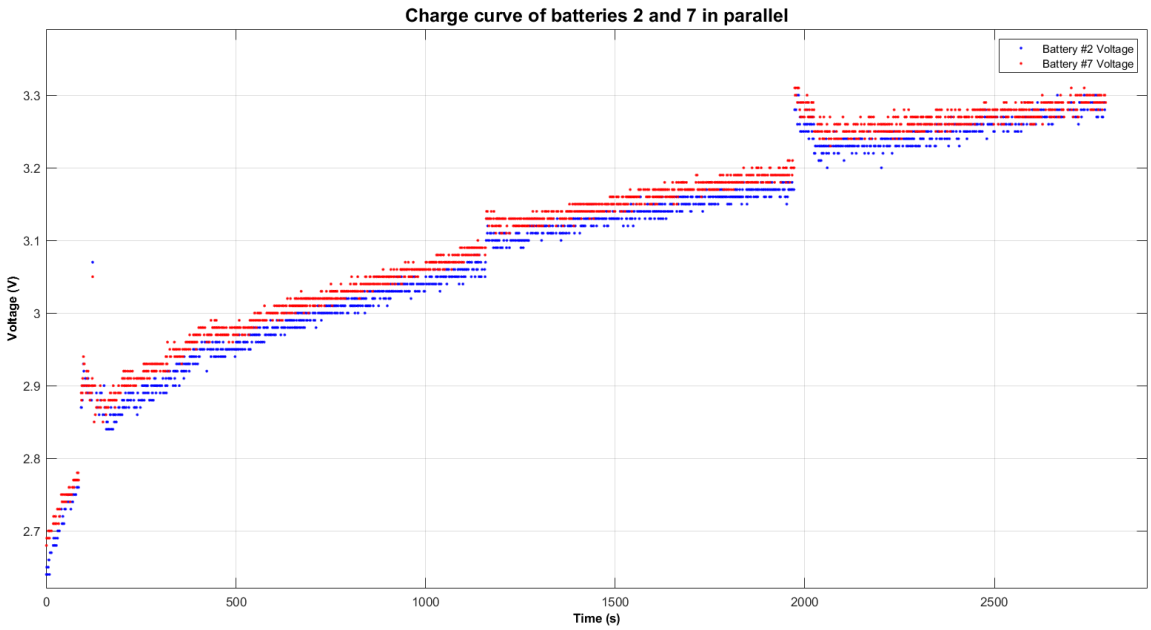

Figure 29. Charge curve of batteries 2 and 7 in parallel

In this case the voltage difference between the two battery cells is lower than the reference in the program (please see flux diagram in 5.3), therefore the microprocessor activates a relay that sets both battery cells in parallel. The charging behavior mirrors that observed in the initial test. However, as both battery cells are charged by the same IC in this scenario, the charging time appears to be shorter. This phenomenon can be explained by analyzing the internal resistance of lithium-ion batteries, following this principle: as the battery voltage decreases, the internal resistance also reduces, thereby providing a higher rate of charge. Furthermore, each battery cell receives a reduced current since the IC provided current is divided between them.

8. Conclusions

- The presented method improves the battery cell parallel balancing capabilities by conserving better battery life and preventing energy loss. This method allows not only a cell balancing but also a full charge of two battery cells simultaneously, which significantly minimizes the energy loss evidenced when balancing two battery cells without charging them before. It allows to measure and plot the voltages of the battery cells and avoids unnecessary charge / discharge cycles that occur when battery cells are connected in parallel as conducted in the preliminary tests.

- The designed system diagnoses battery cell imbalances and takes different actions depending on the status of each battery. When the voltage difference between the battery cells is below a specified reference (see workflow), the microprocessor switches each battery to a charging IC to initiate a full charge cycle. Conversely, when the voltage difference between the battery cells exceeds the specified reference (see workflow), the microprocessor activates the relays, setting both batteries in parallel to either charge them through the same IC or supply a load.

- The relationship between battery voltage and internal resistance significantly influences charging efficiency. Lower battery voltages correspond to reduced internal resistance, allowing for a more efficient charging process. Furthermore, when multiple battery cells are charged using a single IC, the provided current is divided between the cells. This division of current affects the charging rate of each cell, potentially resulting in variations in charge times.

- Voltage source fluctuations and measurement errors, particularly evident at specific points in the charging cycle, can cause anomalies in readings and apparent differences in voltage between cells. Understanding and mitigating these errors are crucial for accurate assessments of the charging process. Using a stable reference, such as Zener diode as a reference source for the microcontroller can potentially remove ADC fluctuations while taking measurements over periods of time.

- After charging and discharging cycles, a relaxation period occurs where the voltage fluctuates before stabilizing. This phase is significant and requires attention, as it influences the overall behavior and stability of the battery cells post-charging, this phase is associated with various electrochemical

processes occurring within the battery. These processes include redistribution of ions within the electrodes and interfaces, structural changes in the materials, and equilibration of chemical reactions.

- Overall, using relays was a satisfactory solution that perfectly isolated the batteries from each other. The time response of the relays did not affect the performance of the system, making them a suitable solution for the objective of this project. However, they had a resistive effect, which altered the voltage output when discharging the circuit in parallel configuration. This effect was more notable when the load had a low impedance.

9. References

[1] Hemavathi S, OVERVIEW OF CELL BALANCING METHODS FOR LI-ION BATTERY TECHNOLOGY, Energy Storage, vol. 3, 2020. [Online]. Available: https://api.semanticscholar.org/CorpusID:225263073

[2] Y. Zhang and S. Lu, RESEARCH ON SERIES-PARALLEL CONNECTION SWITCHING CHARGING METHOD FOR LITHIUM BATTERY OF AUTONOMOUS UNDERWATER VEHICLES, 2018 IEEE 8th International Conference on Underwater System Technology: Theory and Applications (USYS), Wuhan, China, 2018, pp. 1-5, doi: 10.1109/USYS.2018.8779098.

[3] Saurabh Jagtap authored an article titled REVIEW FOR ALGORITHM MODEL OF SWITCHED SHUNT RESISTOR PASSIVE BALANCING TECHNIQUE FOR BATTERY MANAGEMENT SYSTEM, published in the International Journal of Innovative Research in Technology (IJIRT), Volume 7, Issue 1, June 2020, pages 785, ISSN 2349-6002.

[4] Y. Ye, K. W. E. Cheng, Y. C. Fong, X. Xue, and J. Lin, TOPOLOGY, MODELING, AND DESIGN OF SWITCHED-CAPACITOR-BASED CELL BALANCING SYSTEMS AND THEIR BALANCING EXPLORATION, in IEEE Transactions on Power Electronics, vol. 32, no. 6, June 2017.

[5] M. O. Qays, Y. Buswig, M. L. Hossain, M. M. Rahman, and A. Abu-Siada, ACTIVE CELL BALANCING CONTROL STRATEGY FOR PARALLELLY CONNECTED LIFEPO4 BATTERIES, in CSEE Journal of Power and Energy Systems, vol. 7, no. 1, pp. XXX-XXX, January 2021.

[6] Bharti Joshi, Jai Kumar Maherchandani and Abrar Ahmed Chhipa, COMPARISON BETWEEN OPEN AND CLOSED LOOP BATTERY CHARGING TECHNIQUE FOR LITHIUM-ION BATTERY, in International Conference on Electrical Energy Systems (ICEES), vol. 7, February 2021.

[7] Yufeng Zhang, Shaoliang Lu, RESEARCH ON SERIES-PARALLEL CONNECTION SWITCHING CHARGING METHOD FOR LITHIUM BATTERY OF AUTONOMOUS UNDERWATER VEHICLES, in IEEE International Conference on Underwater System Technology: Theory and Applications (USYS), vol. 8, December 2018.

[8] Yuqing Chen, Yuqiong Kang, Yun Zhao, Li Wang, Jilei Liu, Yanxi Li, Zheng Liang, Xiangming He, Xing Li, Naser Tavajohi, Baohua Li. A REVIEW OF LITHIUM-ION BATTERY SAFETY CONCERNS: THE ISSUES, STRATEGIES, AND TESTING STANDARDS, Journal of Energy Chemistry (ELSEVIER), vol. 59, August 2021.

[9] Z. B. Omariba, L. Zhang and D. Sun, "Review of Battery Cell Balancing Methodologies for Optimizing Battery Pack Performance in Electric Vehicles," in IEEE Access, vol. 7, pp. 129335-129352, 2019, doi: 10.1109/ACCESS.2019.2940090.

10. Annexes

10.1 Bill of materials (BOM)

Designator	Name	Description
BT1, BT2	MCP73871T-2CCI_ML	Battery management IC
C1, C3, C5	GRT21BC71H475KE13L	Capacitor 4.7uF
C2, C4, C8	GCM21BD70J106KE02K	Capacitor 10uF
C6	JMK212BBJ476MG-T	Capacitor 47uF
C7	GRM21BR71A225KA01K	Capacitor 2.2uF
D1	BAS116VY-QX	Tripple switching diode
IC1	PIC18F2220-I_SO	Microprocessor
IC2	TPS61027DRCR	DC-DC Converter Boost
J1	USB4140-GF-0170-C	Type-C USB
K1,K2, K3	G6K-2F-DC5	5v Relay
L1	SRP3012CC-6R8M	Inductor 6.8uH
LED1, LED2, LED3	SMLZ24BN3TT86C	Blue LED'
LED10, LED5	HSMW-C170-U0000	White LED
LED11, LED6	APTR3216-VFX	Purple LED
LED4, LED9	SML-S13YTT68	Yellow LED
LED7	SML-S13VTT68	Red LED
LED8	SML-S13MTT68	Green LED
P1	Header 9	Header 9 pins
P2	Header 5	Header 5 pins
P3, P4	Header 4	Header 4 pins
P5, P6	Header 2	Header 2 pins
Q1, Q2, Q3	SMMBT2222ALT1G	BJT Transistor
R1, R15	ERJ-P06F3303V	Resistor 330kΩ
R10,R12, R14, R17, R18, R27, R28, R29, R3, R4, R5	CMP0805AFX-3300ELF	Resistor 330Ω
R11	RCC08054K70FKEA	Resistor 4.7kΩ
R13, R2, R9	RP0805BRD071KL	Resistor 1kΩ
R16	SDR10EZPF1804	Resistor 1.8MΩ
R19, R30	TNPV0805680KBEEA	Resistor 680kΩ
R20, R6	ERJ-P06F1103V	Resistor 110kΩ
R21, R31	TNPV0805180KBEEA	Resistor 180KΩ
R22, R7	ERJ-P06F3302V	Resistor 33kΩ
R23, R8	SDR10EZPF3301	Resistor 3.3kΩ
R24	SG73P2ATTD2003F	Resistor 200kΩ
R25	ERJ-P06J225V	Resistor 2.2MΩ
R26	SDR10EZPF4303	Resistor 430kΩ

10.2 Developed PCB (Altium software)

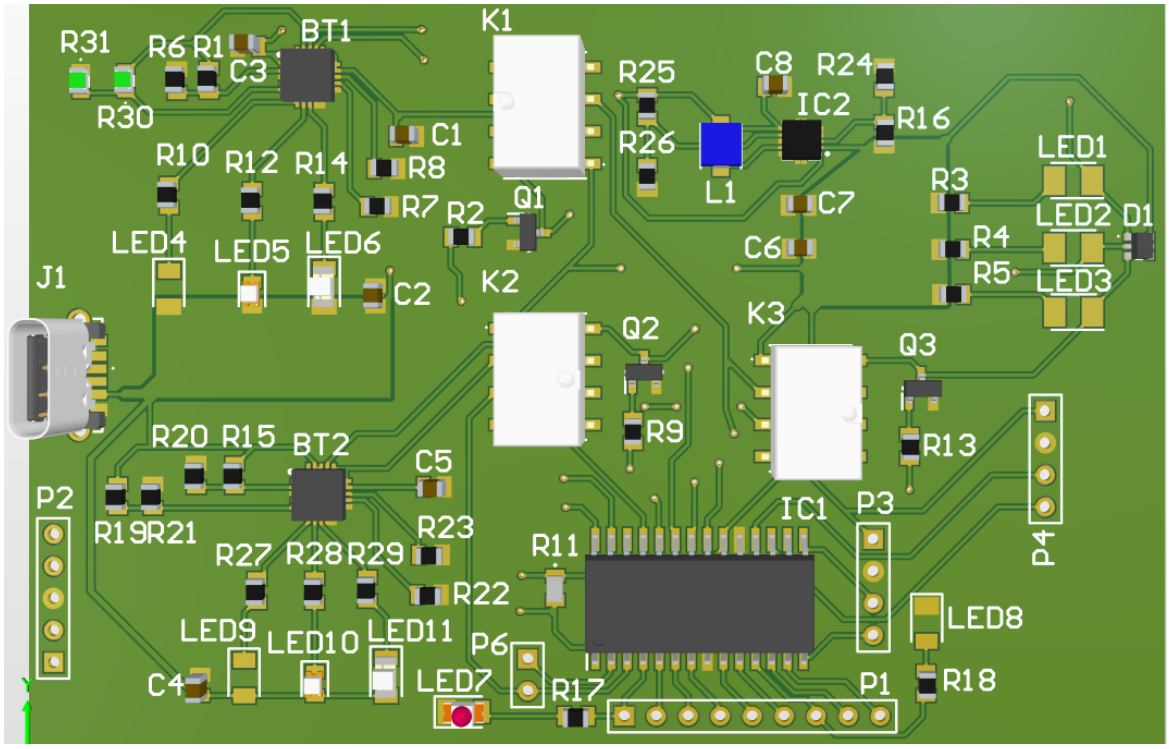

10.3 Developed PCB (Physical board)